Beam hardening errors in post-processing dual energy quantitative computed tomography

Mitchell M. Goodsitt
Department of Radiology, University of Michigan, Ann Arbor, Michigan 48109-0030

(Received 30 November 1994; accepted for publication 18 April 1995)

A computer simulation study was performed to assess the errors due to x-ray beam hardening in the fat and bone estimates of a post-processing dual-energy quantitative computed tomography technique. The "central" calibration method was employed in which calibration standards are inserted within a torso phantom of a size similar to that of the "patient." Although beam hardening errors are reduced with this method, they still occur as a result of mismatches between the *torso* phantom and *patient* body sizes. Two mismatch situations were investigated. In one, a single *torso* phantom was used for all subject sizes (*i.e., one-size-fits-all*). In the other, closest matches were made from a set of three different sized torso phantoms (small, medium, and large). In all cases, the compositions of the calibration standards that were inserted into the torso phantoms consisted of bone, fat (glycerol trioleate), and an average fat-free red marrow. Fifteen patient sizes were simulated ranging from 20 to 34 cm in diameter. There were 21 patients of each size. The vertebrae in these subjects contained known amounts of bone mixed in marrows of composition determined from chemical analyses of cadaver marrow samples. Vertebrae consisting of mixtures of the calibration standard materials were also studied. The computed effective x-ray beam energies at the vertebra location for the various subject sizes ranged from 54.3 to 56.4 keV at 80 kVp and from 74.4 to 78.8 keV at 140 kVp. Maximum root mean square errors due to beam hardening were 1.2 mg/ml bone and 0.007 mass fraction fat for *one-size fits-all* central calibration, and 0.31 mg/ml bone and 0.002 mass fraction fat for *closest match* central calibration. These errors are two to four times smaller than the *maximum* beam hardening errors obtained when the calibration standards and vertebrae are made of identical materials. This study indicates that for a realistic situation in which the compositions of the calibration standards and patient's marrow differ to some extent, the contribution of beam hardening to the overall error in fat and bone estimates is small. Furthermore, these errors can be minimized through the use of a central calibration technique in which a closest match to the patient's body size is made from a set of three different sized torso phantoms.

Key words: bone, computed tomography, beam hardening, dual-energy CT, fat

I. INTRODUCTION

X-ray beam hardening is a common source of error in quantitative computed tomography (CT).[1] Beam hardening is the increase in the effective energy of polyenergetic x-ray beam as it passes through tissue due to the preferential attenuation of low energy x rays. CT numbers of tissues are directly related to the linear x-ray attenuation coefficients of the tissues, which decrease as the effective energy of the x-ray beam increases. Consequently, the (nonbeam hardening corrected) CT number of a tissue at a particular location in a scan decreases as the amount and attenuation of the intervening tissue increases. For quantitative CT measurements of bone mineral density (BMD), calibration standards containing known concentrations of bone mineral or bone mineral equivalent material are usually placed underneath the subject's back and scanned simultaneously with the subject. The beam hardening at the calibration standard and vertebra locations will be different due to the different amounts of intervening tissues, and unless corrections are employed, there will be errors in the computed bone mineral densities. This probability is not that important an issue in conventional single-energy quantitative CT in which subjects are studied longitudinally and the changes in BMD are more significant than the absolute values. However, it can be detrimental even in this case if the subject's body size changes significantly between measurements. The errors may be more important for a post-processing dual-energy quantitative CT (DEQCT) technique that we have been developing for measuring the bone and fat content of vertebrae.[2–5] The propagation of errors associated with utilizing two independent CT number measurements in the dual-energy technique make the technique more susceptible to the effects of small CT number inaccuracies. Although several sophisticated methods for correcting beam hardening errors have been proposed,[6–9] to my knowledge, only very simple beam hardening corrections have been implemented commercially. The purpose of the present study was to estimate the magnitude of the x-ray beam hardening error for our DEQCT technique. I did so both for the ideal case in which the compositions of the materials in the calibration standards and vertebrae are perfectly matched and for the more realistic case in which I employed measured vertebrae marrow compositions which were variable and therefore could not be perfectly matched by the marrow composition used in the calibration standards.

 0094-2405/95/22(7)/1039/9/$6.00

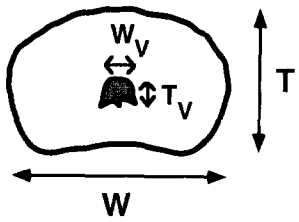

FIG. 1. Sketch depicting human subject dimensions measured in CT slices. T=AP thickness of subject's body, W=width of subject's body, T_V=AP thickness of vertebra, W_V=width of vertebra.

II. MATERIALS AND METHODS

Our DEQCT technique has been described previously.[2–5] In brief, it computes the bone concentration and fat volume fraction of the spongiosa region of a vertebra from the measured mean CT numbers of that region and of a set of calibration standards at two effective x-ray energies. The calibration standards are made of materials that simulate the x-ray attenuation properties of bone, fat, and an average fat-free red marrow.[5]

To minimize the effects of beam hardening and other field nonuniformities, we have favored implementing the DEQCT technique using central calibration—a method in which calibration standards are scanned within a vertebral slot of a patient simulating torso phantom.[2,10] Although the central calibration method reduces beam hardening errors, it does not necessarily eliminate them due to mismatches between the x-ray attenuation properties and sizes and shapes of the torso phantoms and patients.

For the present study, I performed a computer simulation investigation to determine the beam hardening errors resulting from mismatches between the sizes of the calibration torso phantom(s) and the patients. Details of the computer simulation follow.

A. Patient and torso phantom sizes

To determine an appropriate range of patient and torso phantom sizes, I examined CT images of 46 normal human subjects enrolled in QCT studies. Measurements of the widths and anterior–posterior (AP) thicknesses of the subjects' bodies (see Fig. 1) were made in a total of 91 axial slices, 45 containing vertebra T12, and 46 containing L3. The widths and AP thicknesses of the vertebrae excluding the transverse and spinous processes were also measured. Results are summarized in Table I.

To simplify matters, I decided to simulate the patient's bodies with cylinders. Average diameters of these cylinders were computed for each slice using the equation $D=(W+T)/2$, where W=width and T=AP thickness of the body. A similar calculation was performed for the vertebrae in the slices. Relevant statistics for the equivalent diameters of the bodies and vertebrae are contained in Table I.

Torso phantom calibration. For the simulation study, I wished to compare results for two alternative methods of central calibration. In one, a single torso phantom was employed to cover all patient sizes. This is akin to one-size-fits all. In the other, a closest match was made from a set of three different sized torso phantoms (i.e., small, medium, and large). Based on the equivalent cylindrical diameters listed in Table I, I chose a total of 15 patient diameters ranging from 20 to 34 cm, with increments of 1 cm. The one-size-fits all torso phantom had a diameter in the middle of this range (27 cm). One of the set of three torso phantoms had a 22-cm diameter and was used for patients whose diameters ranged from 20 to 24 cm. The second had a 27-cm diameter covering patient sizes 25 to 29 cm, and the third had a diameter of 32 cm, covering patient sizes of 30 to 34 cm. The vertebra in each case was chosen to have a diameter equal to the average equivalent vertebral diameter for all subjects, 3.2 cm.

B. Compositions of spongiosas and calibration standards and subject configurations

In a previous study,[5] we determined the chemical compositions of marrow samples extruded from 21 human cadaver vertebrae. We performed a computer simulation of the DEQCT technique using calibration standards made of bone as defined by Woodard and White,[11] fat (glycerol trioleate), and an average fat-free marrow determined from 12 of the above mentioned marrow samples. The elemental compositions of these standards are: bone:H(3.4), C(15.5), N(4.2), O(43.5), Na(0.1), Mg(0.2), P(10.3), S(0.3), Ca(22.5); fat: H(11.84), C(77.32), O(10.84), and average fat-free red marrow: H(10.35), C(8.11), N(1.82), O(78.90), Na(0.19), Mg(0.03), P(0.08), S(0.11), Cl(0.19), K(0.02), Ca(0.16), Fe(0.05), where the values in parentheses are percentages by

TABLE I. Dimensions of bodies, vertebrae, and equivalent cylinders determined from 91 CT images of human subjects.

	Width of patient body in axial slice (cm)	AP thickness of patient body in axial slice (cm)	Width of vertebra in axial slice (cm)	AP thickness of vertebra in axial slice (cm)	Equivalent cylinder diameters for patient bodies (cm)	Equivalent cylinder diameters for vertebrae (cm)
Minimum	23.6	14.7	2.8	2.1	20.0	2.4
Maximum	40.3	29.3	4.6	3.6	32.4	4.0
Mean	29.2	20.3	3.6	2.8	24.8	3.2
Standard deviation	3.0	2.8	0.4	0.3	2.5	0.3

weight. The mass densities are 1.92 g/ml for bone, 0.92 g/ml for fat, and 1.034 g/ml for average fat-free red marrow.

For the present study, the DEQCT technique was again employed to estimate the bone and fat contents of simulated vertebral spongiosas containing the same 21 marrow samples. However, in this case, these estimates were made for each of the 15 patient dimensions (21 marrows×15=315 estimates). Both one-size-fits-all and closest match central calibration methods were applied using the bone, fat, and average fat-free marrow standards. Furthermore, estimates were made for two spongiosa bone contents—100 mg/ml (58-mg/ml mineral) simulating an osteoporotic individual and 200 mg/ml (116-mg/ml mineral) simulating a normal individual.

In addition, estimates were computed for the situation in which the patients' spongiosas were made of exactly the same components as the calibration standards (bone, fat, and average fat-free marrow). The majority of the 21 human cadaver vertebrae marrow samples that were analyzed previously had mass fractions of fat between 0.1 and 0.6.[5] This same range was covered in this situation. A total of 26 vertebrae were simulated with fat differentials of 0.02 (e.g., marrow fat mass fraction=0.10, 0.12, 0.14,...,0.60). Again results were computed for the two different central calibration techniques, the 15 subject sizes, and the two bone concentrations.

C. Computation of equivalent energies and CT numbers

The CT numbers of the spongiosas and calibration standards that are employed in the DEQCT calculations depend upon the effective x-ray energies at those sites. These energies in turn depend upon the incident x-ray spectra, and the x-ray attenuation of the body tissues. For this study, the x-ray spectra of a GE 9800 CT scanner operated in dual-energy mode at 80 and 140 kVp were estimated using the computer program XSPECW2 which was obtained from Robert Jennings, Ph.D. of the Center for Devices and Radiological Health (U. S. Food and Drug Administration, Rockville, Maryland). The x-ray tube was assumed to have an anode angle of 7 deg, 2.5-mm aluminum inherent filtration, and added filtration of 0.05-mm molybdenum plus 4-mm Teflon, X-ray energies were estimated by calculating the local energy fluence attenuation coefficients as suggested by McCullough.[12] These attenuation coefficients represent the fractional change in the total energy of the polyenergetic spectrum per unit area per unit path length at a point of interest. For this simulation study, these attenuation coefficients were computed at the center of a 3.2-cm diameter vertebra made of 100-mg/ml K_2HPO_4, a bone mineral simulating material. This vertebra was at the center of the patients' bodies which were 20- to 34-cm diameter cylinders made of water. The equation employed for computing the local energy fluence attenuation coefficient was

$$\mu = -\frac{d\psi}{dx}\frac{}{\psi},$$

where x is the thickness variable, and ψ is the integrated *local* energy fluence of the x-ray spectrum.[12] More specifically, $\psi = \int \psi_E \, dE$, and $\psi_E = E\phi_E$, where E is the photon energy at the beginning of each energy interval, and ϕ_E is the spectrally distributed photon fluence (photons/area-energy interval).[12]

The effective energies corresponding with each μ were then determined by logarithmic—logarithmic interpolation within a table of the linear attenuation coefficient of 100-mg/ml K_2HPO_4 in water as a function of x-ray energy ($\Delta E = 1.0$ keV). The linear attenuation coefficients were calculated from the mass attenuation coefficients, μ/ρ, and the concentrations of K_2HPO_4 and water. The mass attenuation coefficients were computed with the program XCOM, which was written by Berger and Hubbel of the National Bureau of Standards, and the concentration of K_2HPO_4 and water were 0.1 and 0.98 g/ml,[13] respectively. It should be noted that although 100-mg/ml K_2HPO_4 is not a perfect simulator for each of the spongiosas studied, it represents the vertebra of an average subject, and permitted the calculation of 30 effective energies corresponding to the 15 body sizes and two x-ray beam kVps. Had separate calculations been performed for each individual spongiosa and calibration standard, about 648 effective energies (2 kVps×15 body sizes×21 vertebrae plus 2 kVps×3 calibration materials×3 torso phantom sizes) would have been required. This would have increased the complexity and computation time of the simulation study significantly.

The DEQCT technique computation requires the input of the CT numbers of the calibration standards and spongiosas at the appropriate effective x-ray energies. These CT numbers were determined by first using the XCOM program to compute the mass attenuation coefficients of water and the principal calibration standard and spongiosa components (e.g., bone, fat, average fat-free marrow, individual subject's marrow) at these energies. The conventional CT number equation was employed:

$$\mathrm{CT\#}(E)_{\mathrm{substance}} = 1000 \times \frac{\mu(E)_{\mathrm{substance}} - \mu(E)_{\mathrm{water}}}{\mu(E)_{\mathrm{water}}}.$$

For example, the CT number of a subject's spongiosa at energy E was computed from

$$\mathrm{CT\#}_{\mathrm{spongiosa}}(E) = 1000 \times \frac{\left(\frac{\mu}{\rho}(E)\right)_{\mathrm{bone}} \times c_{\mathrm{bone}} + \left(\frac{\mu}{\rho}(E)\right)_{\mathrm{marrow}} \times c_{\mathrm{marrow}} - \mu(E)_{\mathrm{water}}}{\mu(E)_{\mathrm{water}}},$$

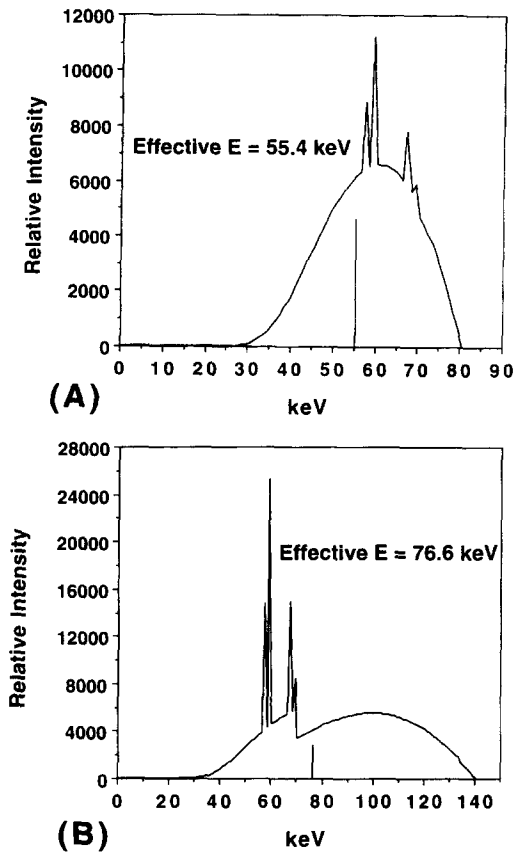

FIG. 2. Examples of computed 80 kVp (A) and 140 kVP (B) spectra passing through the center of a 100 mg/ml K_2HPO_4 in water vertebra. For this particular case, the vertebra was located at the center of a 27-cm diameter simulated subject made of water. The computed effective energies were 55.4 and 76.6 keV and are indicated by vertical lines in the figure.

where c_{bone} is the known concentration of bone—either 0.1 g/ml (100 mg/ml) or 0.2 g/ml (200 mg/ml). c_{marrow} is given by the equation

$$c_{marrow}=\rho_{marrow}\times\left(1-\frac{c_{bone}}{\rho_{bone}}\right),$$

where ρ_{marrow} is the density of the marrow computed from its water, fat, protein, and mineral compositions.[5]

D. Computation of true and estimated mass fractions of fat

The true mass fractions of fat in the spongiosas ($Fat_{spongiosa}$) including bone were given by the equation

$$Fat_{spongiosa}=Fat_{marrow}\times\frac{c_{marrow}}{\rho_{spongiosa}},$$

where Fat_{marrow} is the mass fraction of fat in the subject's marrow by itself, $\rho_{spongiosa}=c_{bone}+c_{marrow}$, and c_{marrow} is as defined above.

For the situations studied in this investigation, the DEQCT technique solves the set of equation for the volume fraction of fat (F) and the concentration of bone (c_{bone}). To determine the estimated mass fraction of fat to be compared with the "true mass fraction of fat" determined above, I used the equation

$$\text{Estimated mass fraction fat}=\frac{m_{fat}}{m_{spongiosa}}=\frac{F\times\rho_{fat}}{\text{Estimated }\rho_{spongiosa}},$$

where Estimated $\rho_{spongiosa}=B\times\rho_{bone}+R\times\rho_{red}+F\times\rho_{fat}$. B, the estimated volume fraction of bone, is equal to c_{bone}/ρ_{bone}. R, the estimated volume fraction of fat-free ("red") marrow, is given by the equation $R=1.0-F-B$ and ρ_{red}=density of average fat-free marrow=1.034.[5]

E. Computation of root mean square errors and beam hardening errors

I calculated the rms errors of the bone concentration and mass fraction fat estimates at each body size for single and triple central calibration. The general equations employed were

$$\text{rms bone concentration error}=\sqrt{\frac{\Sigma_{i=1}^{21}(\text{estimated mg/ml}_i-\text{true mg/ml}_i)^2}{21}},$$

$$\text{rms mass fraction fat}=\sqrt{\frac{\Sigma_{i=1}^{21}(\text{estimated mass fraction fat}_i-\text{true mass fraction fat}_i)^2}{21}},$$

Note that the errors were calculated for the 21 spongiosas within each body size.

The error due to beam hardening at a given patient body size is simply the difference between the rms error at that size and the rms error at the torso phantom size. Representing this in equations, we have

$$\text{Beam Hardening Fat Error}_{\text{patient size } i}=\text{rms fat fraction error}_{\text{patient size } i}-\text{rms fat fraction error}_{\text{torso phantom size}}$$

and

TABLE II. Effective x-ray energies of the 80 and 140 kVp beams for all simulated subject sizes.

Subject diameter (cm)	Effective energy of 80 kVp x-ray beam (keV)	Effective energy of 140 kVp x-ray beam (keV)
20	54.27	74.37
21	54.44	74.70
22	54.61	75.03
23	54.77	75.35
24	54.93	75.67
25	55.09	75.99
26	55.25	76.31
27	55.40	76.62
28	55.55	76.93
29	55.70	77.24
30	55.84	77.55
31	55.99	77.86
32	56.13	78.16
33	56.27	78.46
34	56.40	78.76

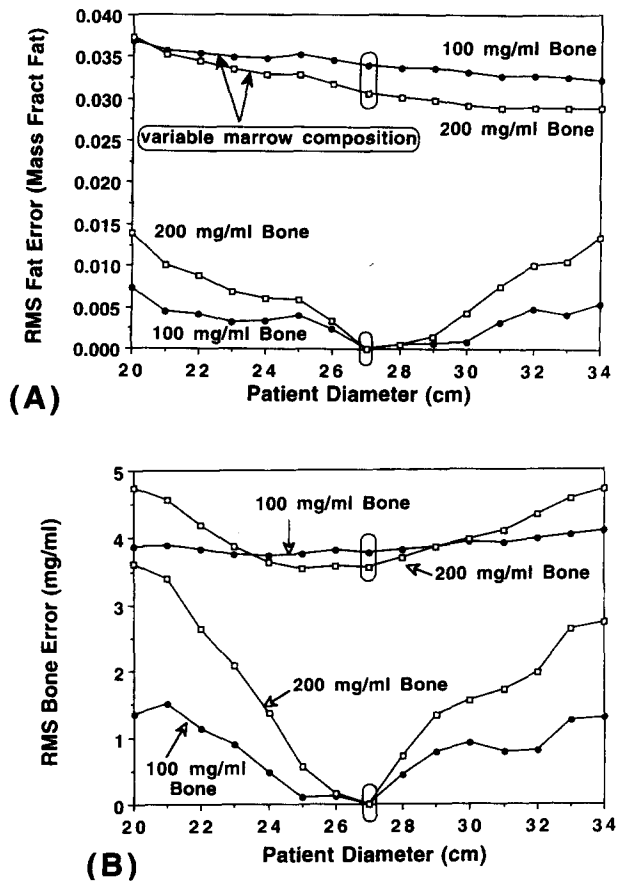

FIG. 3. Root mean square (rms) errors in the fat (A) and bone (B) estimates when the DEQCT technique is implemented using a single (27-cm diameter) central calibration torso phantom for all patient sizes. Plots at the top are for the cases in which the subjects' spongiosas have variable marrow compositions which can not be perfectly matched by the marrow composition in the marrow calibration standard. Plots at the bottom are for the cases in which the materials in the simulated spongiosas and calibration standards have the same compositions. Data points corresponding to zero beam hardening error (subject size=calibration torso size) are circled in the figure. The beam hardening errors for the lower plots are equal to the rms errors. Beam hardening errors for the upper curves are shown in Fig. 5.

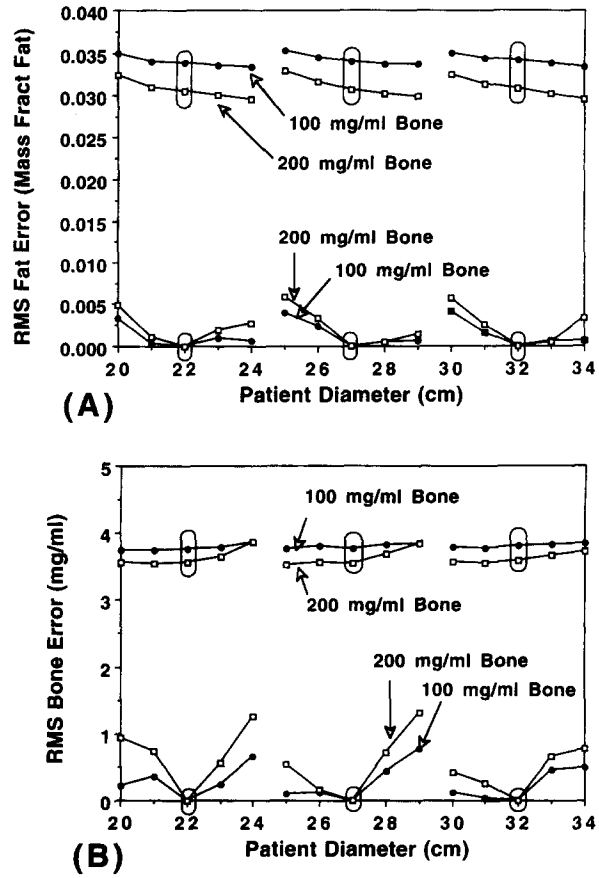

FIG. 4. Root mean square (rms) errors in the fat (A) and bone (B) estimates when the DEQCT technique is implemented using closest match central calibration (either 22-, 27-, or 32-cm diameter torso phantoms). Plots at the top are for the cases in which the patients' spongiosas have variable marrow compositions which cannot be perfectly matched by the marrow composition in the marrow calibration standard. Plots at the bottom are for the cases in which the materials in the simulated spongiosas and calibration standards have the same compositions. Data points corresponding to zero beam hardening error (subject size=calibration torso size) are circled in the figure. The beam hardening errors for the lower plots are equal to the rms errors. Beam hardening errors for the upper curves are shown in Fig. 5.

$$\text{Beam Hardening Bone Error}_{\text{patient size } i} = \text{rms bone concentration error}_{\text{patient size } i} - \text{rms bone concentration error}_{\text{torso phantom size}}.$$

III. RESULTS

Examples of the computed x-ray spectra at the center of the 100-mg/ml K_2HPO_4 solution within one size body phantom are shown in Fig. 2. The effective x-ray beam energies are also indicated in this figure. Table II lists the effective x-ray beam energies for all subject body sizes. The effective energies for the 80-kVp x-ray beam ranged from 54.3 keV for the 20-cm diameter subject to 56.4 keV for the 34-cm diameter subject. The corresponding range for the 140-kVp beam was 74.4 to 78.8 keV. Rms errors in the bone and fat estimates for the perfect and imperfect matches between calibration standard and vertebrae compositions and the two central calibration methods are plotted in Figs. 3 and 4.

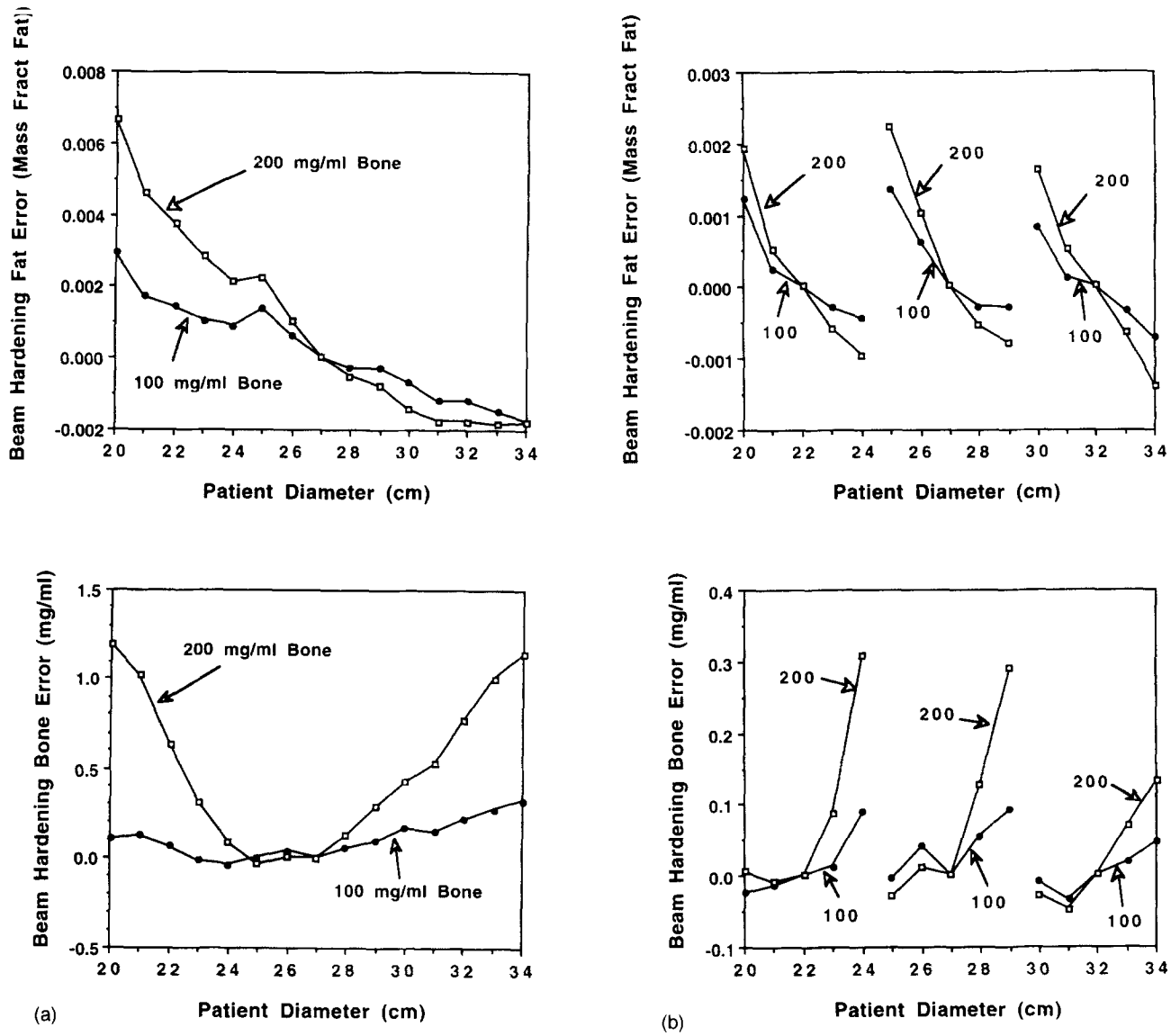

FIG. 5. Beam hardening errors for the case in which there is an imperfect match between the compositions of the materials in the calibration standard inserts and the patients' vertebral spongiosas. The beam hardening error is the differential error due to a mismatch between the size of the patient and the size of the calibration torso phantom. It is computed from the rms error data displayed in Figs. 3 and 4. The beam hardening errors for the one-size-fits-all and closest match central calibration methods are shown in (A) and (B), respectively.

The graphs for the case in which the calibration standards and vertebrae are made of the same materials (the perfect match case) appear at the bottoms of the figures. These graphs pass through 0 rms error, as expected, when the subject and calibration torso phantoms are the same size. Therefore, the rms errors that are displayed in the lower graphs are equal to the beam hardening errors for this situation (see the last two equations in the previous section).

Beam hardening errors for the data displayed in the upper plots in Figs. 3 and 4 are shown in Fig. 5. These were computed using the equations discussed earlier.

IV. DISCUSSION

A. Imperfect match between compositions of materials in standards and spongiosas

The contribution of beam hardening to the error in bone and fat estimates can be assessed by comparing the rms errors for the cases in which the subject dimensions and calibration torso phantom dimensions differ to the case when the dimensions are the same. The latter is a zero beam hardening situation since the x-ray energies at the vertebra and calibration standard sites are identical. The data points associated with zero beam hardening are circled in the figures. The upper curves in Figs. 3 and 4, demonstrate that even without beam hardening, there are errors in the bone and fat estimates when experimentally measured marrow compositions are employed in the subject spongiosas (the case of imperfect match between the compositions of the calibration standards and vertebrae). These errors without beam hardening all ranged between 3.55 and 3.80 mg/ml bone and between 0.030 and 0.034 mass fraction fat.

As shown in Figs. 3 and 4, the above mentioned rms errors changed when beam hardening was present, sometimes for the good—a reduction in rms error, and sometimes

for the bad—an increase in rms error. The reduction in error might at first seem counterintuitive. However, it should be remembered that for the situation at hand, the composition and therefore x-ray attenuation coefficients of the marrow calibration standard do not perfectly match the compositions and x-ray attenuation coefficients of the marrows in the simulated vertebrae. The x-ray attenuation coefficients of each simulated vertebra are further altered relative to those of the calibration standards when the effective energy at the vertebra is different from the effective energy at the calibration standard. The overall result is nonlinear and as seen in the figures, beam hardening is associated with three possible combinations of rms error differentials relative to the zero beam hardening cases. These are as follows: (1) both the fat and bone estimate errors were larger, which was often true when the subjects were smaller than the calibration torso phantom; (2) the fat estimate errors were smaller and the bone estimate errors were larger, which always occurred when the subjects were larger than the calibration torso phantom; and (3) the fat estimates were larger and the bone estimates were smaller, which sometimes occurred when the subjects were smaller than the calibration torso phantom.

For the situation in which the compositions of the simulated patient marrows are determined from chemical analyses of cadaver samples, the maximum beam hardening errors with the *one-size-fits-all* central calibration method were 1.19 mg/ml bone and 0.0067 mass fraction fat [see Fig. 5(a)]. These are the differences between the rms errors for the 20-cm diameter subject /27-cm diameter torso calibration phantom combination (4.75 mg/ml bone; 0.0373 fat) and the rms errors for the 27-cm diameter subject/27-cm diameter torso calibration phantom combination (3.55 mg/ml bone; 0.0306 fat) for the 200 mg/ml bone (normal subject) case. The corresponding maximum beam hardening errors for the closest match central calibration method were 0.31 mg/ml bone and 0.0022 mass fraction fat, again for 200 mg/ml bone case [see Fig. 5(b)]. On the whole, the above values indicate that the errors due to beam hardening, in absolute terms, are small and that closest match central calibration can be used to minimize those errors.

The magnitudes of the rms errors, in general, were smaller for the 200 mg/ml bone cases (see upper curves in Figs. 3 and 4) probably because there was less marrow present in the subject vertebrae (the bone took up more volume). That is, there was less of the material that had a different composition in the vertebrae and calibration standards (the bone and fat compositions were the same). Although the magnitudes of the rms errors were smaller for the 200 mg/ml or normal bone case, the rms error differentials due to beam hardening were actually larger (see Fig. 5).

B. Perfect match between compositions of materials in standards and spongiosas

When the calibration standards and spongiosas are made of the same materials, the results differ from those described above. As shown in the lower plots in Figs. 3 and 4, the DEQCT technique with zero beam hardening (patient size =torso phantom size) now has zero rms error, and beam hardening always results in an increase in rms error. The maximum beam hardening errors for the one-size-fits-all central calibration technique are equal to the maximum rms errors shown in the lower plots in Figs. 3(A) and 3(B), which are 3.61 mg/ml bone and 0.0138 mass fraction fat. For closest match central calibration the maximum beam hardening errors [lower plots in Figs. 4(A) and 4(B)] are 1.32 mg/ml bone and 0.0059 mass fraction fat. These errors are 2.0 to 4.2 times greater than those when there is an imperfect match between the compositions of the standards and the vertebrae (Fig. 5).

Thus the errors arising from variable marrow composition, which would be encountered in human subject studies, minimize the impact of the beam hardening errors. Of course, it should be noted that, in general, the overall absolute rms errors in the estimated bone and fat contents for the imperfect match cases (upper curves in Figs. 3 and 4) are considerably greater than those for the perfect match cases (lower curves in Figs. 3 and 4). It is the relative errors due to difference in the calibration torso and patient body sizes that are smaller for the imperfect match cases.

Finally, another difference between the composition match and mismatch cases is that in the match case, the beam hardening errors are larger for the vertebrae containing 200 mg/ml rather than 100 mg/ml bone. I believe for this situation, the increased error is due to having more bone present, which has a much greater x-ray energy dependence in its x-ray attenuation coefficient than marrow and fat.

C. Beam hardening correction

Most CT scanners employ experimentally measured x-ray transmission values as a function of water thickness to correct the CT projection data for beam hardening. The patient is assumed to be made of water, and the correction works well for most soft tissues since they attenuate x rays similar to water. However, this correction does not work well when the patient contains a significant amount of bone. Then, more sophisticated beam hardening corrections are needed.[6–9]

If the situation that was simulated in this paper were evaluated experimentally with a scanner that employed a first order beam hardening correction, the beam hardening errors would be expected to be even smaller than the simulation estimates. The reason is that the patient and calibration torso bodies were all made of water, which is assumed in the beam hardening correction. There would still be slight beam hardening errors due to the different water equivalent thicknesses of bone in the different sized subjects and phantoms.

D. Beam hardening when subject's body is made of adipose and muscle tissues

For the more realistic situation in which the subject's body is made of adipose and muscle tissues, the beam hardening would be expected to be different. To evaluate the magnitude of this difference, I computed the effective energies of CT scanner x-ray beams traversing bodies containing average amounts of adipose and muscle tissues. I employed the same x-ray spectra and effective energy computation methodology as described previously. The compositions of adipose and muscle tissues were obtained from Woodard and

White,[11] and the XCOM computer program was employed to compute the x-ray attenuation coefficients as a function of energy. Thicknesses of the adipose and muscle tissues in the simulated torsos were determined from information in a paper by Grauer *et al.*[14] This paper indicates that an axial CT scan which passes through the center of the L3 vertebral body of the abdomen of a normal female contains 56% ±16% fat by area, of which 64%±11% is subcutaneous and 36%±11% is intra-abdominal. For the calculation, I assumed the patient's body was cylindrical, that it contained a 3.2-cm diameter vertebra, as before, that there was a 1-cm thick muscle layer between the subcutaneous and intra-abdominal layers, and that the "fat" referred to in the article was actually adipose tissue (a mixture of fat, water, and protein).[11] The computed effective energies of the 80 and 140 kVp x-ray beams for a 20-cm diameter body that is 56% adipose tissue by area were 53.94 and 73.92 keV, respectively. Those for a 34-cm diameter body that is 56% adipose tissue by area were 56.02 and 78.19 keV. When these values are compared with those for water torsos (Table II and further computation), one finds the effective energies for the 20- and 34-cm bodies containing average amounts of adipose and muscle tissues are very similar to those of an 18-cm water phantom (53.92 and 73.71 keV) and a 32-cm water phantom (56.13 and 78.16 keV). These results could be interpreted to mean that one could achieve nearly perfect beam hardening correction if one were to employ a water filled calibration phantom that is on the average 2-cm smaller than the patient. However, it should be remembered that body compositions of subjects vary considerably (e.g., coefficient of variation of total adipose area/total area=16%/56%=29%) and the match with a water phantom may be different for different compositions. Indeed, I have found that if the adipose composition is altered by one standard deviation from the mean, the computed effective energies are significantly altered. Specifically, the effective energies of the 80 and 140 kVp x-ray beams for a 34-cm subject whose body is 72% adipose tissue of which 75% is subcutaneous are 55.72 and 77.72 keV, respectively. From Table II, these values are approximately equal to those of a water torso that is 29 cm in diameter at 80 kVp and 31 cm in diameter at 140 kVp. Central calibration systems which employ adipose and muscle simulating plastics in the torso body and which employ fat rings that are added to the basic phantom to simulate medium and large sized patients, thereby changing the fractional fat area for different body proportions, may solve this problem. Such a system is marketed by CIRS, Inc. (Norfolk, Virginia). The degree to which the CIRS torsos match the beam hardening for a wide variety of human subjects has yet to be established.

E. Effect of cortical rim

Actual vertebrae have an approximately 0.5-mm thick cortical shell which was not simulated in the present study. This shell would result in additional beam hardening errors. However, Hangartner[15] has demonstrated that such errors are minor (e.g., ~1% for single-energy QCT) when scans are obtained on a commercial CT scanner which employs a beam hardening correction (see Fig. 7 of Ref. 15). Furthermore, this contribution to the beam hardening error could be eliminated by incorporating a simulated cortical shall in the calibration torso phantoms.

F. Effect of body shape and vertebral position

In this study, both the subject and the calibration torso phantoms were assumed to be cylindrical in shape with vertebrae or calibration standards located at the centers. Obviously, this will not be the case for clinical studies. The amount of beam hardening in scans of human subjects will be affected by body shape and the position of the vertebra within the body. Use of sophisticated beam hardening corrections and/or calibration torso phantoms that simulate the composition, shape, and vertebral location of human subjects will reduce the beam hardening errors for human subject studies.

V. CONCLUSION

In conclusion, for the realistic situation in which the patient's marrow compositions are variable, and cannot be perfectly matched by the compositions of the calibration standards, the contribution of beam hardening to the overall error in the bone and fat content estimates of a DEQCT technique are small (1.2 mg/ml and 0.007 mass fraction fat at most). A central calibration technique in which the operator selects a calibration torso phantom that is closest to the patient's dimensions from a set of three different sized torsos instead of using one size torso phantom for all patients reduces these errors significantly. Finally, implementation of sophisticated beam hardening corrections in the CT scanner reconstruction algorithm as well as use of calibration torsos containing appropriate amounts of adipose and muscle simulating materials could further limit the errors.

[1]C. E. Cann, "Quantitative CT for determination of bone mineral density: A review," Radiology **166**, 509–522 (1986).
[2]M. M. Goodsitt, D. I. Rosenthal, W. R. Reinus, and J. Coumas, "Two postprocessing CT techniques for determining the composition of trabecular bone," Invest. Radiol. **22**, 209–215 (1987).
[3]M. M. Goodsitt and D. I. Rosenthal, "Quantitative computed tomography scanning for measurement of bone and bone marrow fat content: A comparison of single- and dual-energy techniques using a solid synthetic phantom," Invest. Radiol. **22**, 799–810 (1987).
[4]M. M. Goodsitt, R. H. Johnson, and C. H. Chesnut, "A new set of calibration standards for estimating the fat and mineral content of vertebrae via dual energy QCT," Bone and Mineral **13**, 217–233 (1991).
[5]M. M. Goodsitt, P. Hoover, M. S. Veldee, and S. L. Hsueh, "The composition of bone marrow for a dual-energy quantitative tomography technique: A cadaver and computer simulation study," Invest. Radiol. **29**, 695–704 (1994).
[6]P. M. Joseph, and R. D. Spital, "A method for correcting bone-induced artifacts in computed tomography scanners," J. Comput. Assist. Tomogr. **2**, 100–108 (1978).
[7]D. K. Kijewski and B. E. Bjarngard, "Correction for beam hardening in computed tomography," Med. Phys. **5**, 209–214 (1978).
[8]O. Nalcioglu and R.Y. Lou, "Post-reconstruction method for beam hardening in computerized tomography," Phys. Med. Biol. **24**, 330–340 (1979).
[9]D. D. Robertson and H. K. Huang, "Quantitative bone measurements using x-ray computed tomography with second-order correction," Med. Phys. **13**, 474–479 (1986).
[10]M. M. Goodsitt, R. F. Kilcoyne, R. A. Gutcheck, M. L. Richardson, and

D. I. Rosenthal, "Effect of collagen on bone mineral analysis with CT," Radiology **167**, 787–791 (1988).
[11]H. Q. Woodard and D. R. White, "The composition of body tissues," Brit. J. Radiol. **69**, 1209–1219 (1986).
[12]E. C. McCullough, "Photon attenuation in computed tomography," Med. Phys. **2**, 307–320 (1975).
[13]G. U. Rao, I. Yaghmai, A. O. Wist, and G. Arora, "Systematic errors in bone-mineral measurements by quantitative computed tomography," Med. Phys. **14**, 62–69 (1987).
[14]W. O. Grauer, A. A. Moss, C. E. Cann, and H. I. Goldberg, "Quantification of body fat distribution in the abdomen using computed tomography," Am. J. Clin. Nutr. **39**, 631–637 (1984).
[15]T. N. Hangartner, "Correction of scatter in computed tomography images of bone," Med. Phys. **14**, 335–340 (1987).